Mode assignment for magnetic excitations associated with Co^{2+} impurities in antiferromagnetic FeF_2

David Donnelly
Department of Physics, Sam Houston State University, Huntsville, Texas 77341
(Received 13 February 1995; revised manuscript received 10 April 1995)

We have performed far-infrared (FIR) absorption and Raman-scattering measurements on the Co-FeF_2 system for Co concentrations $0.05 \leq x \leq 5\%$, in magnetic fields $0 \leq H \leq 30$ kG applied parallel to the crystal c axis. In addition to a careful study of the H dependence of the previously reported impurity associated mode at 85 cm^{-1}, we have observed an impurity-induced shift in the host two-magnon FIR absorption, and an impurity-pair excitation in Raman scattering at a frequency of 223 cm^{-1}. Taken together, these results are shown to be inconsistent with the previous interpretation of the 85 cm^{-1} mode as being localized on the impurity spin (i.e., an s_0 mode). Instead, from a mean-field cluster model, we show that the new observations are only consistent with an assignment of the original resonance to be that of a shell mode (s_1). All of the data agrees with this assignment within the framework of the impurity Green's-function theory as well. The 85 cm^{-1} resonance is, to our knowledge, the first s_1 impurity mode to have been observed, a not surprising result when one considers the rather stringent conditions on localization of an s_1 mode contained in Tonegawa's Green's-function theory.

INTRODUCTION

Impurity associated magnetic modes in antiferromagnets have been extensively studied using magnetic resonance,[1] Raman-scattering,[2] or neutron-scattering[3] techniques. The types of modes so studied are gap modes (i.e., modes whose energy is below the $k=0$ magnon energy of the host), local modes (modes whose energy is above the top of the host spin-wave band), and pair excitations (modes made up of two different excitations localized on the same impurity site). In general, these excitations lie in the far-infrared (FIR) region (50–300 cm^{-1}) because of the large effective field acting on the impurity from the exchange coupling to its neighbors. An example of a gap mode is Mn:FeF_2.[4] An example of a local mode is Co:MnF_2.[5] Finally, pair excitations have been observed in Co:MnF_2.[6]

Recently, we have discovered a local mode associated with V impurities in FeF_2.[7] From the field dependence of the linewidth and energy we have been able to identify it unambiguously as the V s_0 mode. Also, from the change in the linewidth of the downgoing branch of the mode as a function of applied field, we have been able to locate the non-s symmetric shell modes localized on the neighboring Fe spins. This was possible because the V s_0 mode did not interact strongly with the host magnons, and passed through the host band without losing its identity. The only change observed in the mode was an increase in its linewidth (and decrease in its lifetime) due to degeneracy with other magnetic modes of the system.

In comparing our results on the V:FeF_2 s_0 mode with an earlier study of an FIR-active mode in Co:FeF_2,[8] we noticed a number of striking differences in the field dependence of the two modes. The two most striking being the g value of the mode, and the degree of interaction of the mode with the host magnetic modes. The earlier study identified the observed mode as the s_0 impurity mode. This prompted us to reexamine the Co:FeF_2 problem from both an experimental and theoretical point of view. The experimental work involves FIR absorption and Raman scattering, and the theoretical work employs mean-field theory and impurity Green's-function techniques. Since the conclusion we have come to is that the Co resonance above the band at 85 cm^{-1} is an s_1 and not an s_0 mode, as was originally thought to be the case, it is necessary to review the theory so as to provide the necessary nomenclature to describe the experimental results and the underlying rationale which makes this new identification so compelling.

THEORY

Host: FeF_2 is a two-sublattice antiferromagnet with the rutile structure. The collinear antiparallel ordering below the Néel temperature ($T_N = 78.2$ K) along the crystal c axis is shown in Fig. 1. The magnetic structure is body-centered tetragonal, with each spin having two nearest neighbors (NN) along the c axis, eight next-nearest neighbors (NNN) at the body corners, and four third-nearest neighbors (3NN) along the x and y axes.

The magnetic part of the Hamiltonian can be expressed

$$H = -2\sum_{i>j} J_{ij}\mathbf{S}_i\cdot\mathbf{S}_j + \sum_i D_i(S_{iz})^2 + \mu_B\mathbf{H}_0\cdot\sum_i g_i\mathbf{S}_i \ , \qquad (1)$$

where J_{ij} is the Heisenberg exchange interaction between spins at sites i and j, and D is the single ion anisotropy. For FeF_2, the dominant exchange interaction J_2 is between next-nearest neighbors (NNN) on opposite sublattices. However, the best fit to the neutron inelastic scattering requires the consideration of three exchange interactions, J_1, J_2, and J_3, where the subscript i denotes

 ©1995 The American Physical Society

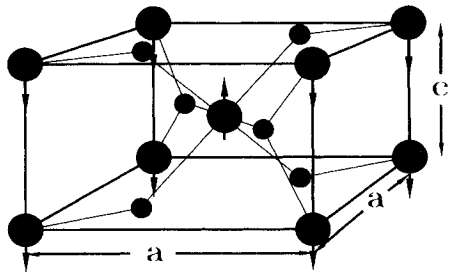

FIG. 1. Rutile crystal structure. Small circles are F^- ions, and large circles are transition-metal ions. Spin alignment at low temperature is also shown.

the ith nearest neighbor.[9] Because $D<0$, the spins align along the easy (c) axis. The Zeeman term describes the interaction of the spins with an external magnetic field H_0.

Using well known spin operator second quantization techniques one can transform Eq. (1) into a spin-wave Hamiltonian whose low-lying collective excitations are characterized by a change in the total spin of the crystal of ± 1. The magnon dispersion relation can be calculated by diagonalizing the Hamiltonian using the usual transformations to Bose creation and annihilation operators.[10] In FeF_2, dispersion has been measured with inelastic neutron scattering,[11] and the values of J_1, J_2, and J_3, and D determined by fitting the theoretical dispersion relation to the data. The energy of the gap at $k=0$ is best determined from antiferromagnetic resonance to be 52.4 cm^{-1}. The energies of the magnons at the zone boundary are directly related to the values of J_1, J_2, J_3, which are $J_1=0.024\pm0.03$ cm^{-1}, $J_2=-1.82\pm0.05$ cm^{-1}, $J_3=-0.097\pm0.03$ cm^{-1}, and $D=-6.46\pm0.15$ cm^{-1}.[9] Because J_1 and J_3 are much smaller than J_2, there is only a slight anisotropy in the magnon energies at the different symmetry points on the Brillouin-zone boundary and to structure in the magnon density of states $N(E)$. For what follows the most important feature is that the magnon energy along (001) is 79.1 cm^{-1} at the top of the band. In the presence of an applied magnetic field, the magnon band splits into two branches, one whose energy increases with increasing field (upgoing) and one whose energy decreases (downgoing).

Experimentally, two aspects of the host magnon FIR absorption spectrum are observed. The first of these is antiferromagnetic resonance (AFMR), the resonance excitation of the $k=0$ magnon which has been extensively studied, and is well understood.[4,12] The second is the two-magnon absorption band which occurs as a result of one photon being absorbed, and two magnons of equal energy and opposite wave vector being created. Because magnons from different parts of the Brillouin zone contribute differently to the two-magnon absorption, it has a rather complicated structure. The mechanism for the two-magnon absorption involves creation of two magnons on adjacent sites in the crystal via the excitation of a virtual electronic state. One feature of the two-magnon absorption which will be important for our purposes later on is the field independence of its energy. Because adjacent Fe sites are on opposite sublattices, the energy of one of the created magnons increases in an applied field by the same amount the energy of the second magnon decreases.

Impurity: When an impurity spin is substituted for a host spin, the spectrum of magnetic excitations changes. In particular, the presence of the impurity breaks the translational symmetry of the crystal, and new modes arise which are associated with the presence of the impurity. The energies and spatial distribution of the impurity associated modes are dependent on the spin and single-ion anisotropy of the impurity, and the exchange interaction between the impurity and the host. Only if the energies lie outside (either above or below) the band of host excitations will the modes be spatially localized on or around the impurity—a necessary though not sufficient condition.

There are several levels of approximations which can be used to calculate the energies of impurity associated modes. The simplest of these is to treat the cluster of the impurity and its exchange coupled host spins in the mean-field approximation. This model assumes that the impurity concentration is low enough that impurities do not interact with each other. In this approximation, each spin precesses in the effective field created by the surrounding spins. In the case of the impurity spin, we may write the effective Hamiltonian as

$$H=-2J_1'\sum_{\gamma}S_{iz}S_{\gamma z}-2J_2'\sum_{\delta}S_{iz}S_{\delta z}+D'(S_{iz})^2 -g\mu_B\mathbf{H}_0\cdot\mathbf{S}_i\ , \tag{2}$$

where the first sum is over nearest neighbors γ coupled to the impurity via J_1', and the second sum is over next nearest neighbors δ coupled to the impurity via J_2'. Also included are the anisotropy and Zeeman terms for the impurity. With the impurities randomly distributed throughout the crystal, there will be equal numbers on both sublattices. Hence, the impurity associated modes will split into two branches in a field H_0 parallel to the c axis of the crystal in the same way as do the host modes. For the excitation localized on the impurity, its energy will vary with H_0 with the g value of the impurity, rather than with that of the host. A Hamiltonian for the cluster of the host spins which are exchange coupled to an impurity will yield a different mode and will have its energy change with the host g value as H_0 is varied.

If the temperature $T\ll T_N$, the spin operators may be replaced by their ground-state expectation values, which, in the Néel state, are just the magnitudes of the spins. There are then two modes associated with the presence of the impurity. The first of these modes is localized on the impurity itself. This is the mode which is usually observed experimentally, and it is referred to as the s_0 mode. The energy of this mode can be determined by assuming that the z component of the impurity spin decreases by 1, and ignoring the effect of transverse-spin components. The energy of the s_0 mode is then given by

$$E_{s0}=-2z_1J_1'S-2z_2J_2'S+(2S'-1)D'\pm g'\mu_BH_0\ , \tag{3}$$

where z_1 is the number of nearest neighbors and z_2 is the number of next-nearest neighbors (two and eight, respectively for FeF_2). We have included in the expression for the energy two host-impurity exchange interactions. For some impurities, however, only one interaction is required.

Because a host spin which has an impurity as a neighbor feels a different effective field than a host spin which has all host neighbors, there is also a second mode which is localized on the neighbors to an impurity. If a single host-impurity exchange between NNN is assumed, the mode will be localized on NNN to an impurity. This mode is referred to as the shell mode, and its energy is given by

$$E_{\text{shell}}=E_{\text{ZB}}+2J_2S-2J_s'S'\pm g\mu_B H_0 \ , \tag{4}$$

where E_{ZB} is the $H_0=0$ energy of a host zone-boundary magnon and is given by

$$E_{\text{ZB}}=-2z_1J_1S-2z_2J_2S+D(S_z)^2 \ . \tag{5}$$

Note again that the energies of the s_0 and shell modes have different field dependence, with the s_0 mode having the g value of the impurity, and the shell mode having the g value of the host. If there is an appreciable difference in the two g values, this fact can be used to determine which spins are involved in a particular excitation. Note also that the shell-mode energy is close to the energy of zone-boundary host magnons, with the difference determined by the difference between host-host and host-impurity exchange.

Because the far-infrared (FIR) driving field is spatially uniform, only individual modes of uniform (s) symmetry can be observed experimentally. However, pair excitations with particular symmetries can also be observed. The pair excitations involve the simultaneous creation of an s_0 mode and a shell mode at the same impurity site by a single photon. The process involved in these excitations is similar to that associated with the host two-magnon absorption in that they proceed via a virtual electronic state. The pair excitations can be observed both in Raman scattering and in FIR absorption. In FIR absorption, a component of the electric field of the incident light must be parallel to the c axis. We can determine the energy of these excitations by assuming that an s_0 mode is excited on the impurity, and that a shell mode is then excited on the neighboring spins. The host spins would see a smaller effective field due to the impurity because the impurity spin has decreased by 1. The energy of the pair excitation is then given by

$$\begin{aligned}E_{\text{pair}}=&-2z_1J_1'S-2z_2J_2'S+(2S'-1)D'+E_{\text{ZB}}\\&+2J_2S-2J_2'(S'-1)\pm(g-g')\mu_B H_0 \ .\end{aligned} \tag{6}$$

While the mean-field cluster approximation gives a good intuitive picture of impurity associated modes, it has some shortcomings. First, this approximation only predicts two (impurity and shell) impurity associated modes whereas from the number of spins in the cluster of $z+1$ (1 impurity and z neighbors) ions one should expect $z+1$ modes. Also, this approximation is rather crude, and is usually only accurate to within 10%. The accuracy becomes even worse as the impurity mode energies approach the energies of the host modes. If accurate predictions are to be made, one must resort to more elaborate methods of calculation.

Much more accurate predictions may be obtained by using the method of impurity Green's functions. This method has been used previously to predict the properties of substitutionally doped anitferromagnets.[13–15] The pure crystal Green's functions are first calculated by decoupling the equations of motion in the random-phase approximation. This reduces the Green's functions to two-spin correlation functions by removing higher-order terms associated with longitudinal spin correlations. The impurity Green's functions are then obtained from the pure crystal Green's functions by assuming that the impurity produces a spatially localized potential. The problem is then reduced to the solution of a secular determinant. For a single host-impurity exchange interaction J_2', this determinant is $(z+1)\times(z+1)=9\times9$. The problem is further simplified by introducing a unitary transformation which block diagonalizes the matrix.[16] The blocks then transform according to various irreducible representations of the impurity point group, and the modes are classified by these representations. For the system under consideration, there are a total of nine impurity associated modes, only two of which are of s symmetry; an s_0 mode localized on the impurity, and an s_1 mode which is localized on the next-nearest neighbors to the impurity. The remainder, all non-s modes, are also localized on the neighbors to the impurity. There are three modes of p symmetry, three of d symmetry, and one of f symmetry. It should be noted again that the energies of all the shell modes are close to the top of the host magnon band, with the energy separation determined by the difference in the host-host and host-impurity exchange interaction.[13,16] The different modes can be pictured semiclassically as precessing spins. The two s-symmetry modes can then be thought of as either the impurity or its eight nearest neighbors precessing in phase. These two modes are shown schematically in Fig. 2.

The impurity Green's-functions technique is particularly useful in establishing the conditions for localization of the various symmetry shell modes as a function of impurity and host parameters (S, S', J_2, J_2', D, and D'). Extensive calculations have been made by Tonegawa,[13] and we directly use his results. Since only s-symmetry

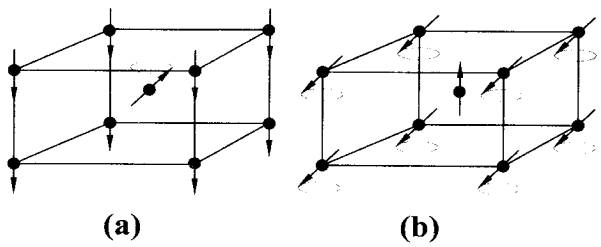

FIG. 2. Schematic representation of s-symmetry modes. (a) Impurity mode, (b) shell mode.

modes may be observed in FIR absorption, we only consider the condition for localization of the s_1 shell mode. (The s_0 mode is assumed to be localized if its energy is outside of the host magnon band.) The condition for localization of the s_1 mode, i.e., for it to appear above the top of the host magnon band, is given by

$$\beta > \frac{1}{(1+\delta+\beta\delta')} ,$$

where

$$\beta = \frac{S'}{S} , \quad \delta = \frac{D}{z_2 J_2} , \quad \delta' = \frac{D'}{z_2 J_2} .$$

Note that this condition does not depend on the size of the host-impurity exchange interaction.[17]

Another result of Tonegawa's calculation is worth noting. If the anisotropy of both the host and impurity are ignored, then there is value of β below which there will never be a localized s_1 mode, regardless of how large is the host-impurity exchange. This result seems at first glance to be somewhat strange, as the mean-field energy of the shell mode depends linearly on the host-impurity exchange. The interpretation of this result is that as the impurity spin gets smaller, or as the s_1 mode energy gets closer to the top of the host magnon band, the s_1 mode becomes more spatially delocalized, eventually becoming indistinguishable from the host modes. From these conditions, one would expect that a special combination of parameters would be required to observe a localized s_1 mode.

EXPERIMENTAL RESULTS

The first experiments performed on the Co:FeF_2 system were the measurement of FIR absorption as a function of applied field at normal incidence with the incident light propagating along the c axis of the crystal. This repeated the earlier measurements.[8] Our measurements were made on a single-crystal sample with a nominal Co concentration of 0.05%. Absorption was measured in fields $0 \leq H \leq 30$ kG using a Bomem DA3.002 Michelson-type Fourier-transform spectrometer. Samples were cooled in a He bath cryostat, which also contained the superconducting solenoid, to $T=6$ K. To improve signal-to-noise ratios, the method of field ratios was used. In this method, the ratio of spectra of different magnetic fields is taken, thereby eliminating any spectral features which do not change with an applied field. A typical ratio spectrum for this sample is shown in Fig. 3. This ratio spectrum is typical of a magnetic impurity mode. The absorption which points up is the mode at $H=0$, while the two absorptions which point down are the two branches of the mode which has split in the applied field.

We observed a uniform impurity associated mode at an energy of 85.0 cm^{-1} at $H=0$, which is ~ 0.5 cm^{-1} lower than the previously published result. There are two possible explanations for this discrepancy. The first is that there is some concentration dependence in the energy of the mode. The previous study was performed on samples

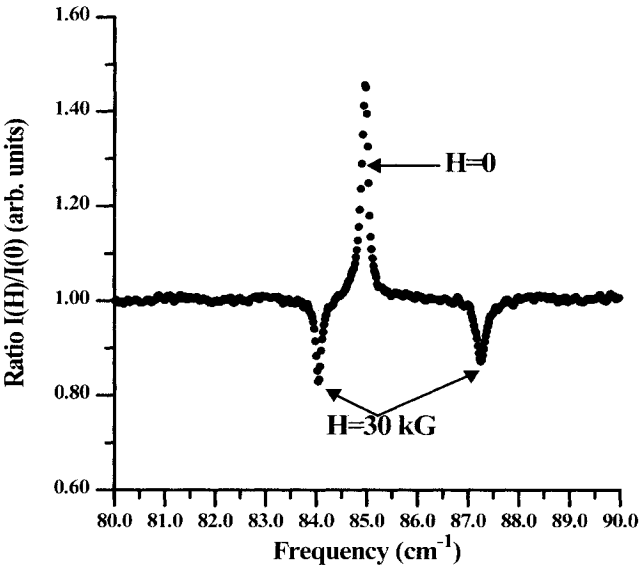

FIG. 3. Ratio spectrum of 0.05% Co:FeF_2. Absorptions at $H=0$ and $H=30$ kG are indicated.

which had a higher Co concentration (0.5–4 %) than the crystals we used. However, no concentration dependence of the mode energy was reported, and in the concentrations we studied (0.05–1 %), we also observed no concentration dependence in the energy. A more plausible explanation for the difference in the zero-field energies is that the frequency calibrations of the two spectrometers used were slightly different. This explanation would also account for a discrepancy in the location of the top of the FeF_2 magnon band in the previous study. The proximity of the mode to the top of the FeF_2 magnon was also intriguing in light of the earlier results on V:FeF_2.

The dependence on applied field of the energy of both branches of the observed mode is shown in Fig. 4. The data from the previous study, along with the results of this study are shown. There are two things to note about the data. First, the energy of neither branch of the observed mode changes linearly with field. Second, the upgoing branch begins to exhibit linear behavior at high fields, but its g value is very close to that of the host ($g_{obs}=2.2$, $g_{FeF_2}=2.22$). This value is very different from the g values for Co^{2+} ions measured in similar octahedrally coordinated F^- environments [$g=3.2$ for Co s_0 mode in MnF_2,[18] $g=4.1$ for Co^{2+} electron paramagnetic resonance (EPR) in ZnF_2,[19] $g=4.24$ for Co^{2+} EPR in MgF_2,[20] and $g=2.8$ for CoF_2 AFMR (Ref. 21)]. The fact that the g value of the mode is so close to that of the host and so different from that of the impurity suggests that the mode is localized on Fe spins rather than on the Co impurities. This would make it an s_1 shell mode rather than the usual s_0 impurity mode.

Further support of this conjecture is found in the strong interaction of the mode with the host zone-boundary magnons. The downgoing branch of the im-

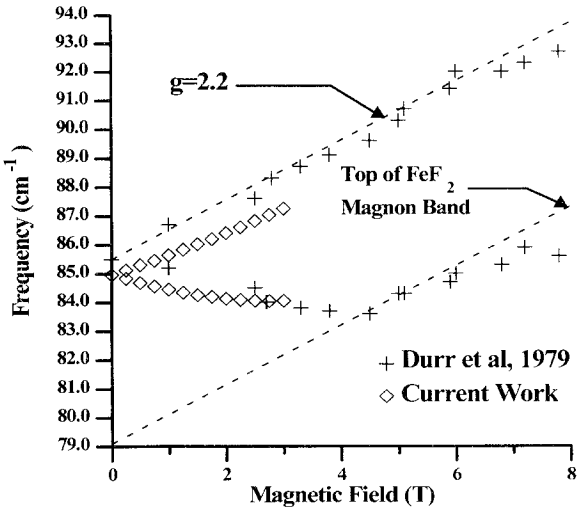

FIG. 4. Frequency vs field for Co:FeF_2 mode. Previous work along with results of current study is shown. Top of FeF_2 magnon band and g value of upgoing branch are also shown.

purity mode actually exhibits anticrossing, increasing its energy with applied field at high fields. The interaction also affects the host magnons. This effect is visible in an induced field dependence of the FeF_2 two-magnon absorption. Recall that in pure FeF_2, the two-magnon absorption is independent of applied field. However, while looking for pair modes in a 45° geometry where both the wave vector of the incident light and the applied magnetic field were at 45° angle to the c axis, an "artifact" appeared in the ratio spectrum at an energy of ~ 160 cm^{-1}. A ratio spectrum showing this artifact is shown in Fig. 5(a). Note that this ratio spectrum does not look like the ratio spectrum of an impurity associated mode, as there are not two field-dependent branches. However, this is evidence that something is changing when a magnetic field is applied. Closer examination reveals that the energy of this "artifact" is on the high-energy side of the FeF_2 two-magnon absorption. Recall that the two-magnon absorption is caused by the creation of two magnons of equal and opposite wave vector by a single magnon. This effect is normally independent of any applied magnetic field, but the presence of Co impurities causes it to change. A transmittance spectrum showing the two-magnon absorption is shown in Fig. 5(b). Close examination revealed that the "artifact" observed in the ratio spectra was indeed caused by a small change in the shape of the two-magnon absorption. This effect was observed at Co concentrations as low as 1%.

To further test the hypothesis that the observed mode was the s_1 mode, we first performed Raman-scattering experiments on the Co:FeF_2 system in an effort to observe impurity-pair excitations. These modes have been observed in similar systems using both Raman-scattering[22] and FIR absorption.[2] Incident light was provided by the 514 nm line of an Ar^+ ion laser, and the scattered light was detected with a double monochromator using a cooled, photon counting photomultiplier. The Raman spectrum of a sample with a nominal Co concentration of 0.5% was measured. The sample was cooled in a He bath cryostat to a temperature of 4.5 K, and frequency shifts between 40 and 500 cm^{-1} were scanned.

Along with the phonon and magnon peaks which are usually observed in FeF_2, an additional peak was observed at a frequency shift of 223 cm^{-1} which was not present in pure FeF_2. The Raman spectrum of this peak is shown in Fig. 6(a). Because there is a Raman-active

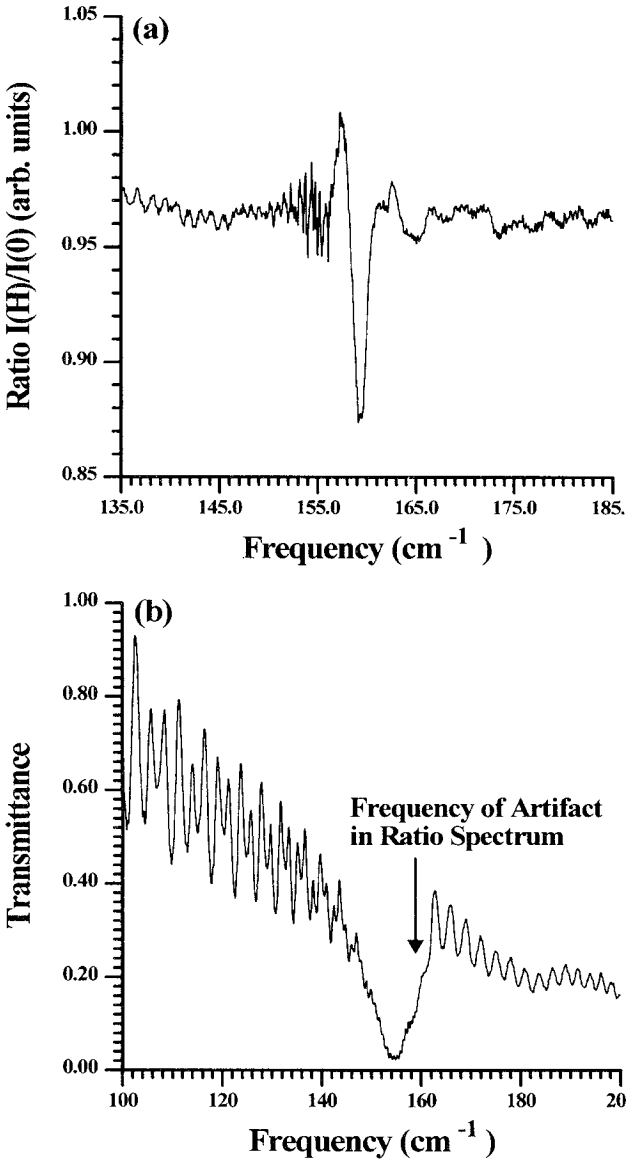

FIG. 5. (a) Ratio spectrum of 3% Co:FeF_2 taken in 45° geometry. Spectra at $H=0$ and $H=30$ kG are used. Artifact is clearly visible. (b) Transmittance of 3% Co:FeF_2 taken in 45° geometry. Two-magnon absorption is visible, and energy of artifact in ratio spectrum is also indicated. Note that horizontal scale is different than in (a).

phonon in FeF_2 at 257 cm^{-1}, the possibility that the observed line was a vibrational impurity mode needed to be considered. One way of determining this would be to measure any shift of the line in an applied field. However, we were not able to apply a magnetic field in the Raman-scattering experiment, so we needed to find another method of determining if the observed line was magnetic or vibrational in nature. Fortunately, the Debye temperature in FeF_2 is quite high, and the phonons can still be observed at room temperature. The Néel temperature is much lower, however, and any magnetic excitations will have completely disappeared when the sample has reached temperatures around 50 K. The temperature dependence of the observed line should then reveal whether it is vibrational or magnetic in nature.

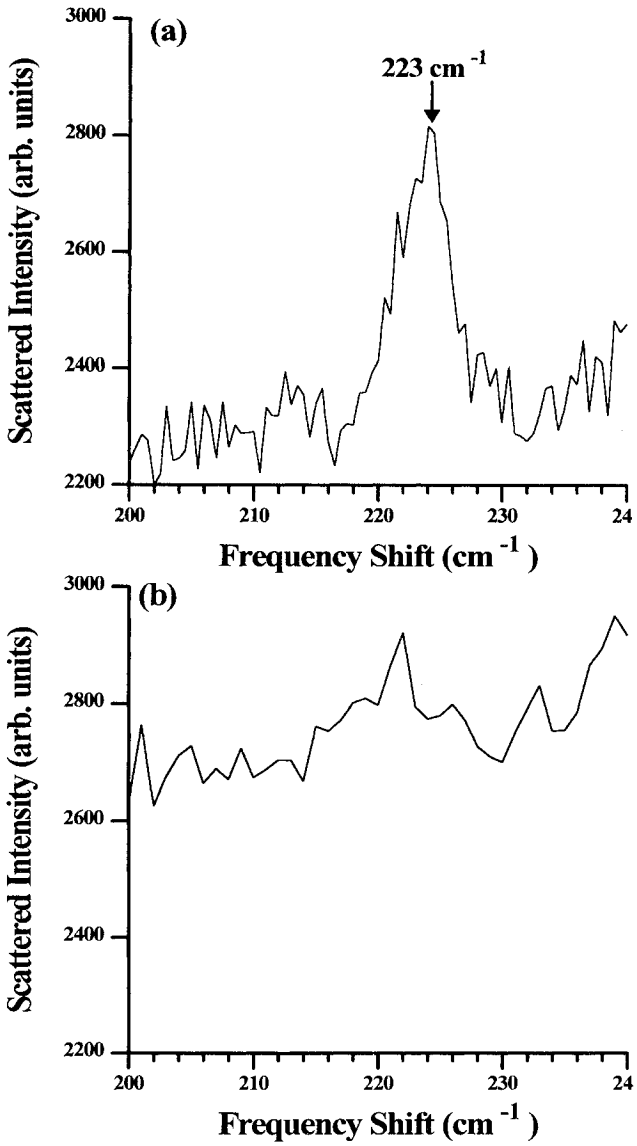

FIG. 6. Raman spectrum of 0.5% Co:FeF_2 (a) $T=4.5$ K. (b) $T=50$ K. Energy of impurity associated peak is indicated.

Raman spectra were measured for temperatures between 4.5 and 50 K. Both the impurity associated line and the Raman-active phonon at ~ 260 cm^{-1} were monitored to observe any difference in the temperature dependence. The Raman spectrum of the impurity associated line at a temperature of 50 K is shown in Fig. 6(b). Note that at 50 K, the impurity line is barely visible, while no change was observed in the phonon at 257 cm^{-1} over the same temperature range.

The temperature dependence of the Raman line leads us to conclude that it is magnetic in nature. The logical conclusion is that it is the impurity-pair excitation mentioned above. These excitations are caused by the simultaneous excitation of a local impurity mode and a shell mode by a single photon. Because Raman scattering proceeds without a change of parity, and the Co ground state is an odd parity state,[23] both s_0-p and s_0-f modes should be visible. Because of the low resolution of the spectrometer, we only observed a single line. Attempts to observe both uniform impurity modes and pair excitations in FIR absorption were hindered by the presence of the FeF_2 reststrahl band, which extends upward from 155 cm^{-1}.

DISCUSSION

This observed shift in the two-magnon absorption is caused by the interaction of the downgoing branch of the observed impurity mode at 85 cm^{-1} with top of the upgoing FeF_2 magnon band. This shift occurs in the following way: The impurity interacts strongly with the host magnons, exhibiting anticrossing effects. It is reasonable to assume that the host magnons behave similarly. Since the impurity mode only interacts with one host magnon branch, the two branches no longer change their energies by the same amount, and the two-magnon absorption is thereby affected.

This affect raises the question of how only 1% of the spins in the crystal can have such a large effect on the host modes. If the mode were an s_0 mode, one does not expect that this would happen, because the mode should be localized mainly on the impurity, even for mode energies close to the top of the host magnon band. Such localization has been observed in the V:FeF_2 system where the s_0 mode occurs at frequency of 83.0 cm^{-1}.[7] We resolve this dilemma by concluding that there are more spins than just the impurity spins participating in the excitation. This can only be the case if the excitation is localized on host spins rather than on impurity spins. In fact, if the excitation were the s_1 shell mode, then there would be eight times as many spins participating in the excitation, and its spatial extent would be larger. This makes the observed effect on the host spins more plausible.

The energies of the s_0 and shell modes can be predicted from the pair mode energy using mean-field theory. Assuming a single host-impurity exchange interaction between NNN, and using $S=2$, $S'=1.5$, $D=6.5$ cm^{-1},[9] and $D'=26.3$ cm^{-1},[24] we get a value of the host-impurity exchange of

$$J_{2\text{Fe-Co}} = -3.35 \text{ cm}^{-1} .$$

We then can calculate the energies of the s_0 and shell modes using this value. The energies are

$$E_{s0} = 159.7 \text{ cm}^{-1} \text{ and } E_{\text{shell}} = 85.0 \text{ cm}^{-1} .$$

These numbers are in surprisingly good agreement with experiment. The proximity of the s_0 mode to the FeF_2 reststrahl band makes observation difficult.

Finally, we turn to the localization conditions discussed earlier. We can apply these conditions to this system to determine if a localized s_1 mode is to be expected. If we use the parameters appropriate to Co:FeF_2, namely $D = 6.5 \text{ cm}^{-1}$,[3] $D' = 26.3 \text{ cm}^{-1}$,[24] $S' = 1.5$, $S = 2$, we find that

$$\frac{1}{(1+\delta+\beta\delta')} = 0.357 < \beta = 0.75$$

and a localized s_1 mode is indeed expected.

CONCLUSION

We have repeated the earlier study, and have performed additional experiments which form a detailed study of the Co:FeF_2 system. We have determined that the previous interpretation was incorrect, and that the observed mode at 85 cm^{-1} is the s_1 shell mode rather than the s_0 impurity mode. Support for this conclusion is as follows: (a) The observed mode is very close in energy to the top of the FeF_2 magnon band. This is not conclusive proof, but we know that shell modes are always close to the top of the host magnon band. (b) The g value of the mode is very close to that of the host, and very different from Co^{2+} in similar environments. (c) The observed mode interacts very strongly with host magnons, contrary to observed behavior of other s_0 modes (7). (d) The energy of the pair excitation is inconsistent with the observed mode being an s_0 mode. If the observed were an s_0 mode, one would estimate the pair excitation energy to be the sum of the energies of the top of the host magnon band and the s_0 mode (around 160 cm^{-1}). The presence of the pair mode at 223 cm^{-1} requires a much larger s_0 mode energy.

The previous interpretation was based on a calculation by Weber[25] which determined impurity mode eigenvectors for a linear chain when the mode was located either above or below the host band. The calculation showed that at zero field, the spatial extent of the impurity mode was inversely proportional to the energy separation from the host band. As the spatial extent of the mode becomes larger, there are more host spins participating, and this reasoning was used to explain the observed g value of the mode.

However, when a magnetic field is present, Weber's arguments no longer apply. The mode will spread spatially only as it gets closer to the host band of the same polarization (e.g., a downgoing impurity mode gets closer to the downgoing host band). This can only happen under very special circumstances. When the impurity mode and the host band it is approaching are of opposite polarizations, more elaborate mechanisms for coupling must be invoked. The mechanism for decay of impurity modes into host modes of the opposite polarization has been studied theoretically,[13] and proceeds via S_z nonconserving interactions. So, the arguments used to explain the previously observed behavior are not valid in this case.

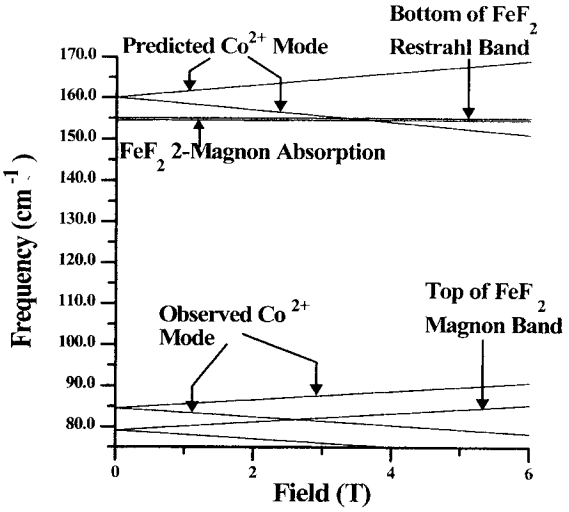

FIG. 7. Energy-level diagram for Co:FeF_2 system. Frequencies of relevant host modes, as well as observed and predicted Co modes are indicated.

The observed behavior is exactly what one would expect if the observed mode were an s_1 shell mode, however. First, the mode would be localized on host spins, so that the expected g value would be that of the host. Also, since the s_1 mode is similar to the modes at the zone boundary, one would expect it to interact strongly even with host modes of the opposite polarization. Finally, as the s_1 mode approaches the host band, it becomes more spread out spatially, and it becomes more like the host modes with which it is degenerate, so that its intensity should decrease, as is observed.[8]

While the s_0 mode has not yet been observed in this system, its energy has been predicted to be $\sim 160 \text{ cm}^{-1}$. This is very close in energy to the FeF_2 reststrahl band, which makes observation of it difficult. Application of a high enough magnetic field might drive the downgoing branch below the reststrahl band. Also, the mode might be observed in reflectance measurements. Efforts are underway to observe this mode. An energy-level diagram for this system is shown in Fig. 7.

ACKNOWLEDGMENTS

The author wishes to thank D. Hone and V. Jaccarino for helpful discussions, and gratefully acknowledges support by Research Corporation.

[1]M. Butler, V. Jaccarino, N. Kaplan, and H. J. Guggenheim, Phys. Rev. B **1**, 3058 (1970).
[2]G. Parisot, S. J. Allen, R. E. Dietz, H. J. Guggenheim, R. Moyal, P. Moch, and C. Dugautier, J. Appl. Phys. **41**, 890 (1970).
[3]W. J. L. Buyers, T. M. Holden, E. C. Svensson, R. A. Cowley, and R. W. H. Stevenson, Phys. Rev. Lett. **27**, 1442 (1971).
[4]R. W. Sanders, Ph.D. thesis, U. C. Santa Barbara, 1978.
[5]W. J. L. Buyers, R. A. Cowley, T. M. Holden, and R. W. H. Stevenson, J. Appl. Phys. **39**, 1118 (1968).
[6]R. E. Deitz, G. Parisot, A. E. Meixner, and H. J. Guggenheim, J. Appl. Phys. **41**, 888 (1970).
[7]D. Donnelly, D. Hone, and V. Jaccarino, Phys. Rev. Lett. **65**, 2286 (1990).
[8]U. Durr and B. Uwira, J. Phys. C **12**, L793 (1979).
[9]H. J. Guggenheim, M. Hutchings, and B. Rainford, J. Appl. Phys. **39**, 1120 (1968).
[10]C. Kittel, *Quantum Theory of Solids* (Wiley, New York, 1963).
[11]M. T. Hutchings, B. D. Rainford, and H. J. Guggenheim, J. Phys. C **3**, 307 (1969).
[12]R. M. Toussaint, Ph. D. thesis, U. C. Santa Barbara, 1982.
[13]T. Tonegawa, Prog. Theor. Phys. **40**, 1195 (1968).
[14]P. Thayamballi and D. Hone, Phys. Rev. B **27**, 2924 (1983).
[15]S. M. Rezende, Phys. Rev. B **27**, 3032 (1983).
[16]E. Shiles and D. Hone, J. Phys. Soc. Jpn. **28**, 51 (1970).
[17]Tonegawa also calculated a more stringent condition which does depend on the strength of the exchange, but the calculation was done assuming only a single exchange interaction for both the host and the impurity, and as was stated above, three exchange interactions are needed to accurately model the host behavior, so that the more stringent condition is really only a first approximation.
[18]R. Weber, J. Appl. Phys. **40**, 995 (1969).
[19]M. Tinkham, Proc. R. Soc. London, Ser. A **236**, 535 (1956).
[20]H. M. Gladney, Phys. Rev. **146**, 253 (1966).
[21]P. L. Richards, J. Appl. Phys. **35**, 850 (1964).
[22]A. Oseroff and P. S. Pershan, Phys. Rev. Lett. **21**, 1593 (1968).
[23]H. M. Gladney, Phys. Rev. **146**, 253 (1966).
[24]M. E. Lines, Phys. Rev. **137**, A982 (1965).
[25]R. Weber, Z. Phys. **223**, 299 (1969).